



Wong, C. Y., Martinez, J., Zhao, J., Al-Salami, H., & Dass, C. R. (2020). Development of orally administered insulin-loaded polymeric-oligonucleotide nanoparticles: statistical optimization and physicochemical characterization. *Drug Development and Industrial Pharmacy*. <https://doi.org/10.1080/03639045.2020.1788061>

Peer reviewed version

Link to published version (if available):  
[10.1080/03639045.2020.1788061](https://doi.org/10.1080/03639045.2020.1788061)

[Link to publication record in Explore Bristol Research](#)  
PDF-document

This is the author accepted manuscript (AAM). The final published version (version of record) is available online via Taylor and Francis at <https://www.tandfonline.com/doi/full/10.1080/03639045.2020.1788061>. Please refer to any applicable terms of use of the publisher.

## University of Bristol - Explore Bristol Research

### General rights

This document is made available in accordance with publisher policies. Please cite only the published version using the reference above. Full terms of use are available:  
<http://www.bristol.ac.uk/red/research-policy/pure/user-guides/ebr-terms/>



## Development of orally administered insulin-loaded polymeric-oligonucleotide nanoparticles: statistical optimization and physicochemical characterization

Chun Y. Wong, Jorge Martinez, Jian Zhao, Hani Al-Salami & Crispin R. Dass

To cite this article: Chun Y. Wong, Jorge Martinez, Jian Zhao, Hani Al-Salami & Crispin R. Dass (2020): Development of orally administered insulin-loaded polymeric-oligonucleotide nanoparticles: statistical optimization and physicochemical characterization, Drug Development and Industrial Pharmacy, DOI: [10.1080/03639045.2020.1788061](https://doi.org/10.1080/03639045.2020.1788061)

To link to this article: <https://doi.org/10.1080/03639045.2020.1788061>



Accepted author version posted online: 28 Jun 2020.



Submit your article to this journal [↗](#)



View related articles [↗](#)



View Crossmark data [↗](#)

# Development of orally administered insulin-loaded polymeric-oligonucleotide nanoparticles: statistical optimization and physicochemical characterization

Chun Y. Wong<sup>a,b</sup>, Jorge Martinez<sup>a</sup>, Jian Zhao<sup>c,d,e</sup>, Hani Al-Salami<sup>f</sup>, Crispin R. Dass<sup>a,b,\*</sup>

<sup>a</sup>*School of Pharmacy and Biomedical Sciences, Curtin University, Bentley 6102, Australia*

<sup>b</sup>*Curtin Health Innovation Research Institute, Bentley 6102, Australia*

<sup>c</sup>*MRC Integrative Epidemiology Unit, University of Bristol, Bristol, UK*

<sup>d</sup>*NIHR Bristol Biomedical Research Centre, University of Bristol, Bristol, UK*

<sup>e</sup>*Population Health Sciences, Bristol Medical School, University of Bristol, Bristol, UK*

<sup>f</sup>*Biotechnology and Drug Development Research Laboratory, School of Pharmacy and Biomedical Sciences, Curtin Health Innovation Research Institute, Bentley 6102, Australia*

## **OCID:**

Chun Y. Wong: <https://orcid.org/0000-0001-6132-6432>

Hani Al-Salami: <https://orcid.org/0000-0003-0049-6969>

Crispin R. Dass: <https://orcid.org/0000-0001-7087-7957>

## **\* Corresponding author:**

**Mail** | Professor Crispin R. Dass,  
School of Pharmacy and Biomedical Sciences,  
Curtin University,  
GPO Box U1987,  
Perth 6845,  
Australia.

**Email** | [Crispin.Dass@curtin.edu.au](mailto:Crispin.Dass@curtin.edu.au)

**Phone** | +61 8 9266 1489

**Running title:** Evaluation of oligonucleotide-polymeric nanoparticles

**Key words:** chitosan, insulin, nanoparticles, oligonucleotide, polymer, protein

## Abstract

**Introduction:** Therapeutic peptides are administered *via* parenteral route due to poor absorption in the gastrointestinal (GI) tract, instability in gastric acid and GI enzymes. Polymeric drug delivery systems have achieved significant interest in pharmaceutical research due to its feasibility in protecting proteins, tissue targeting and controlled drug release pattern.

**Materials and Methods:** In the present study, the size, polydispersity index and zeta potential of insulin-loaded nanoparticles were characterized by dynamic light scattering and laser doppler micro-electrophoresis. The main and interaction effects of chitosan concentration and Dz13Scr concentration on the physicochemical properties of the prepared insulin-loaded nanoparticles (size, polydispersity index and zeta potential) were evaluated statistically using Analysis of Variance. A robust procedure of reversed-phase high-performance liquid chromatography was developed to quantify insulin release in simulated GI buffer.

**Results and Discussion:** We reported on the effect of two independent parameters, including polymer concentration and oligonucleotide concentration, on the physical characteristics of particles. Chitosan concentration was significant in predicting the size of insulin-loaded CS-Dz13Scr particles. In terms of zeta potential, both chitosan concentration and squared term of chitosan were significant factors that affect the surface charge of particles, which was attributed to the availability of positively-charged amino groups during interaction with negatively-charged Dz13Scr. The excipients used in this study could fabricate nanoparticles with negligible toxicity in GI cells and skeletal muscle cells. The developed formulation could conserve the physicochemical properties after being stored for 1 month at 4 °C.

**Conclusion:** The obtained results revealed satisfactory results for insulin-loaded CS-Dz13Scr nanoparticles (159.3 nm, pdi 0.331, -1.08 mV). No such similar study has been reported to date to identify the main and interactive significance of the above parameters for the characterization of insulin-loaded polymeric-oligonucleotide nanoparticles. This research is of importance for the understanding and development of protein-loaded nanoparticles for oral delivery.

## 1. Introduction

Oral drug administration is deemed to be a patient acceptable, convenient and safe route [1]. However, therapeutic peptides are administered *via* parenteral route due to poor absorption in the gastrointestinal (GI) tract, instability in gastric acid and GI enzymes [2]. Subcutaneous injections of therapeutic agents cause a number of negative clinical implications, for instance, occasional overdose, inconvenience due to multiple daily administration, and local skin adverse effects. Recently, sub-micron sized drug delivery systems have achieved significant interest in pharmaceutical research due to its feasibility in tissue targeting and controlled drug release pattern. A substantial quantity of studies have been carried out to investigate the potential of empty polymeric nanoparticles [3,4] and microparticles [5] in disease management, and their secondary roles in encapsulation of drugs, peptides, vaccines, cells and genes. The majority of the recent pharmaceutical research defines "nanoparticles" and "microparticles" as particles with size smaller and larger than 1  $\mu\text{m}$  respectively. It was suggested that particles with size greater than 5  $\mu\text{m}$  remain in the Peyer's patches, nevertheless particles with size smaller than 10  $\mu\text{m}$  can be transported across the efferent lymphatics [6]. Nevertheless, oral administration of various therapeutic agents *via* polymeric nano- and microcarriers remain unsuccessful. The challenges that restrict the sub-micron sized drug formulations from reaching the blood circulation include large particle size, instability in the GI tract, and inappropriate zeta potential for GI penetration and retention [7].

Owing to the large molecular weight, insulin molecules cannot diffuse across the GI tract [8,9]. In the present study, positively-charged chitosan and negatively-charged scrambled Dz13 sequence (Dz13Scr) were used to fabricate the insulin-loaded nanoparticles [10]. With the use of chitosan-based nanoparticles, previous studies revealed that the GI permeation and oral bioavailability of therapeutic proteins could be improved due to the opening of tight junctions [9,11]. Chitosan is a natural polymer that can be acquired from partial deacetylation of chitin, which is obtained from crustacean shell, fungi and yeast [12]. Chitosan offers several advantages as it is one of the most abundant natural, biodegradable, hydrophilic, biocompatible, mucoadhesive, safe and non-allergenic polymers [13]. Its high stability in the GI tract has gained significant attention in the development of oral nano-formulations such as BSA-loaded nanoparticles [14,15], insulin-loaded nanoparticles [15-17], cryptdin-2-loaded nanoparticles [18], iron-lactoferrin-loaded nanoparticles [19-23], hepatocyte growth factor-loaded nanoparticles [24], and granulocyte colony-stimulating factor [25]. Oligochitosan, which is a naturally degraded product of chitosan, can preserve the favourable characteristics of chitosan and has been used to prepare insulin-loaded decanoic acid-grafted oligochitosan nanoparticles. The nanoparticles that were prepared by oligochitosan could

lower the blood sugar level, present low toxicity *in vivo* and facilitate the transportation of insulin across the GI tract. Pure chitosan nanoparticles and microparticles demonstrated beneficial effects including suppression of gastric [26] and liver cancer cells, inhibition of bacterial growth [27], and immune response regulation [28]. When therapeutic agents were entrapped in chitosan nanoparticles and microparticles [29], they were found to be effective in targeting breast cancer cells [30], management of blood sugar level [31], and diuresis [32]. Chitosan and its derivatives was also effective in activating immune response, suppressing tumour growth [33], stimulating cytokine production [34,35] and forming circulating antibody [36]. A substantial number of research articles report the effectiveness of chitosan-based nanoparticles in cancer [37,38] by promotion of immune response, or a reduction in side-effects when co-administered with monoclonal antibodies [39].

Dz13 is a DNzyme that has been reported to be effective in inducing apoptosis, suppressing angiogenesis activity of various tumour cells and neointima formation [40]. It can resist exonuclease degradation due to 3'-3' linked nucleotide modification [41,42]. Dz13 is not stable in the mouse and human serum [43]. Such limitation may have negative impacts on the stability of parenteral formulations, but not the development of orally administered nanoparticles as the entrapped drugs should be released from the destabilised drug delivery system for GI absorption. Dz13 and Dz13Scr (scrambled Dz13 sequence or catalytically inactive form of Dz13) were stated to be harmless to normal healthy cells [44]. They are deemed to be non-toxic and non-immunogenic gene-silencing agents [45]. Both *in vitro* and *in vivo* studies demonstrated that Dz13 and Dz13Scr did not elicit the activation of innate immune cells [46-48]. In clinical trial, Dz13 and Dz13Scr were well tolerated and patients did not present any serious adverse events [49]. One of the previous studies reported that doxorubicin-loaded Dz13 or Dz13Scr nanoparticles were safe *in vivo* with minimal toxicity in normal cells for clinical management of bone cancer [44]. Upon storage of the chitosan-Dz13 nanoparticles, the formulation could maintain its stability for at least 1 month [43].

According to the database from U.S. National Library of Medicine (that is, ClinicalTrials.gov database), to date, only two parenteral protein-based nanoformulations, including RSV-F protein nanoparticle vaccine and albumin-bound rapamycin, have been examined in clinical trials [50]. Previous review indicated that at least 100 insulin-loaded nanoparticulate formulations have been developed in the previous two decades [10]. However, the clinical translation of orally administered protein-based nanoparticles remains unsuccessful, and none of the formulations have been approved by the Food and Drug Administration [51]. Hence, there is a need to explore the use of novel excipients and their potential in developing orally administered insulin-loaded nanoparticles. In this study, encapsulation of insulin within the CS-Dz13Scr nano- and microcarriers was carried out.

Peptide encapsulation in sub-micron sized drug delivery system was suggested to be one of the approaches in increasing the oral bioavailability of the therapeutic agents. An extensive number of *in vitro* studies reported that biopolymers such as chitosan and alginate could withstand enzymatic degradation in the GI tract [10]. Table 1 illustrate the insulin-loaded nanoparticulate formulations that have previously adopted the mathematical approaches to evaluate the physicochemical properties and understand the formulation characteristics. These formulations include insulin-loaded poly (3-hydroxybutyrate-co-3-hydroxyvalerate) nanoparticles [52], lyophilized insulin-loaded N, N-dimethyl-N-octyl chitosan nanoparticles [53], lyophilized insulin-loaded modified chitosan nanoparticles [8], insulin-loaded chitosan/arabic gum nanoparticles [12,54], insulin-loaded modified chitosan nanoparticles [55], insulin-loaded chitosan/albumin-coated alginate/dextran nanoparticles [56], and insulin-loaded poly-epsilon-caprolactone/ Eudragit RS1 nanoparticles [57]. Currently, there is no comprehensive research available on the physicochemical characterization and statistical evaluation of insulin-loaded polymer-oligonucleotide nanoparticles.

In our experiments, complex coacervation was used for particle synthesis. Compared to modified solvent emulsification-evaporation method [58] and nanoprecipitation [59], the technique used in the study do not involve organic solvents and sonication that are harmful to labile therapeutic agents. Statistical evaluation was used to examine the effect of individual independent variables as well as their mutual interactions on the experimental response of insulin-loaded nanoparticles [55,60-62]. The relationship between independent variables and outcome of drug formulation can be visualised by response surface plots. The effect of the following critical variables, including polymer concentration and oligonucleotide concentration, on the formation of particles were investigated. This statistical evaluation provided an insight in the developmental stage, for instance, the main independent effects, interaction effects and quadratic effects, of polymeric-oligonucleotide nanoparticulate formulations. The stability of the formulation was examined by the conservation of physicochemical properties and fourier-transform infrared spectroscopy (FTIR) after the nanoparticles were being stored for 1 month. The encapsulation efficiency and drug release profile of insulin were analysed by reversed-phase high-performance liquid chromatography (RP-HPLC). Last but not least, the cytotoxicity of the developed formulation was characterized.

## **2. Materials and methods**

### **2.1 Materials**

Low molecular weight (LMW) chitosan (95% deacetylated; MW 150 kDa) and Dz13Scr were obtained from Sigma-Aldrich (St Louis, MO, USA). Insulin was purchased from Gibco (Fort Worth, TX, USA). Trifluoroacetic acid (Sigma-Aldrich), acetonitrile (Thermofisher, VIC, Australia) and Milli-Q water used in the experiments were of pharmaceutical and analytical grade.

### **2.2 RP-HPLC for insulin testing**

The protocol for insulin quantification was developed using a Shimadzu HPLC LC-20AT system (Kyoto, Japan) coupled with a UV-Vis detector [63,64]. The chromatographic runs were operated using Apollo C18 column (Maryland, USA) with 5  $\mu$ m particle size (4.6 mm inner diameter  $\times$  150 mm length) at a flow rate of 1 mL/min. The UV-Vis detection wavelength was 214 nm. The mobile phase consisted of solution A (Milli-Q water) and solution B (0.1% TFA in acetonitrile). The gradient elution of solution B was pumped from 10 to 90% in 9 minutes. A stock insulin solution of 1.2 mg/mL was freshly prepared using Milli-Q water. The stock solution was used for the preparation of 8 standard solutions at concentrations of 2.97, 6.06, 12.13, 24.25, 48.5, 80.81, 121.25, and 202.06  $\mu$ g/mL. A calibration curve was drawn by plotting the peak areas of each standard solution against the known insulin concentration.

### **2.3 Preparation of insulin-loaded CS-Dz13Scr nanoparticles**

Insulin-loaded CS-Dz13Scr nanoparticles were manufactured by vortex-assisted complex coacervation [65-67]. In this study, insulin stock solution (20.9  $\mu$ M) was prepared by dissolving the powder in Milli-Q water, followed by subsequent dilution to 100 nM by Milli-Q water. Then, 100  $\mu$ L insulin (100 nM) was added to an equal volume of Dz13Scr (5, 10 or 15  $\mu$ g; in 50 mM SS buffer, pH 6.15) with gentle mixing. Then, chitosan solution (0.00004, 0.00025, 0.0004, 0.0025, 0.004, 0.025, 0.04 or 0.25%; in 25 mM SA buffer, pH 7) was added. The following experimental conditions, including microfuge tube size (600  $\mu$ L), preparation time (30 second) and speed (40 Hertz), were used to prepare the insulin-loaded nanoparticles. Before storing the samples in the fridge at 4  $^{\circ}$ C for further experimentation, 30 minutes were allocated for insulin-loaded CS-Dz13Scr nanoparticles/microparticles to stabilize. All samples were prepared in triplicates for physical characterization and statistical evaluation. The experiments were repeated for at least one



time. **Figure 1** is a schematic diagram illustrating the steps for the preparation and pharmaceutical analysis of insulin-loaded CS-Dz13Scr nanoparticles.

## **2.4 Physicochemical characterization of insulin-loaded nanoparticles**

### **2.4.1 Particle size and polydispersity index measurement**

The size and polydispersity index of formulated nanoparticles were examined. Prior to measurement, samples were kept in the fridge at 4 °C. An ideal formulation should consist of small (<500 nm) and uniform particles to facilitate mucosal absorption and enhance drug bioavailability. In this study, the mean size of the prepared particles was determined by dynamic light scattering [2,68]. A scattering angle of 90° was used to measure the particle size. The results were reported as mean ± SD. The homogeneity of the formulated particles was also determined.

### **2.4.2 Zeta-potential measurement**

The zeta-potential of the prepared particles were determined using laser doppler micro-electrophoresis using a Zetasizer ZSP (Malvern Instruments Ltd., UK) [69,70]. Samples were prepared in triplicates for measurement and the experiment was repeated for at least one time. In brief, 300 µL of nanoparticles or microparticles were suspended in 300 µL sterile Milli-Q water at room temperature, followed by filling in the folded capillary cell (DTS1070). The electric field strength of 5 V/cm was used to record the zeta potential at room temperature. The data was generated by Zetasizer software (Version 7.11). The results were reported as mean ± SD.

## **2.5 Statistical evaluation of insulin-loaded nanoparticles**

According to previous literature (**Table 1**), the concentration of nanoparticle excipients, such as polyvinyl alcohol [52] and N-dimethyl-N-octyl chitosan [53], are considered to be critical independent variables that can influence the physicochemical properties (e.g. particle size, polydispersity index) of nanoparticles. The effect of independent variables (polymer concentration as  $X_1$ , oligonucleotide concentration as  $X_2$ ) on the response variables (size as  $Y_1$ , polydispersity index as  $Y_2$  and zeta potential as  $Y_3$ ) was examined. Insulin-loaded nanoparticles were prepared according to all combination of chitosan concentration (0.00004, 0.00025, 0.0004, 0.0025, 0.004, 0.025, 0.04 or 0.25%) and Dz13Scr concentration (5, 10 or 15 µg) in triplicates. After preparation of insulin-loaded nanoparticles, the response variables were obtained by using dynamic light

scattering and laser doppler micro-electrophoresis as mentioned previously ( $n = 3$ ). We fitted the data using a linear model with quadratic polynomial terms, where the main and interaction effects of (polymer concentration and oligonucleotide concentration) on response variables (size, polydispersity index and zeta potential) were estimated. A coefficient of determination ( $R^2$ ) was also estimated to illustrate how much variation of the response variables was explained by these independent variables [8,52,53]. The model goodness of fit was assessed by  $R^2$  and lack of fit value. P-value less than 0.05 was used as statistical significance threshold for assessing effect sizes estimated using Analysis of Variance (ANOVA) in Design-Expert 10. The formulated equation is considered to be acceptable with no significant lack of fit (p-value > 0.05). Three-dimensional surface response plots were drawn to illuminate the association between independent variables and dependent experimental responses in a graphical manner. These diagrams are valuable in clarifying the relationship between the input variables and outcome of interest.

## **2.6 Conservation of the physicochemical properties**

As 0.004% chitosan (in 25 mM SA buffer) and 10  $\mu$ g of Dz13Scr (in 50 mM SS buffer) could produce insulin-loaded nanoparticles with the smallest particle size and reasonable polydispersity index, such combination was selected for further investigation in stability analysis, FTIR analysis, morphology examination, encapsulation efficiency analysis, drug release study and cytotoxicity examination. To determine the stability of the developed insulin-loaded nanoparticles, the formulation was stored at 4 °C for 1 month. The physicochemical properties of the nanoparticles, including particle size, polydispersity index and zeta potential, were assessed after being stored for 1 month.

## **2.7 Fourier transform infrared (FTIR) spectroscopic analysis**

ATR-FTIR analysis (FTIR spectrometer spectrum two with UATR two accessory, Perkin-Elmer, Buckinghamshire, England) was conducted by scanning the samples from 4000 to 450  $\text{cm}^{-1}$  at room temperature [63,71-76]. The spectra of 100 nM insulin, 100 nM of insulin-loaded CS-Dz13Scr nanoparticles, and 100 nM of insulin-loaded CS-Dz13Scr nanoparticles (after 1-month storage) were obtained using the attenuated total reflection (ATR) mode at room temperature. The characteristic peaks of insulin and insulin-loaded nanoparticles were examined to evaluate the stability of the formulation as well as the interaction between insulin and excipients in the formulation [52]. The in-built software (Spectrum, Perkin-Elmer) was utilized for double subtraction [8] and ATR correction.

## 2.8 Morphological characterization

The morphology of the insulin-loaded CS-Dz13Scr nanoparticles was examined by scanning electron microscopy (Zeiss Neon 40EsB, Germany) at 3kV. Prior to scanning, the nanoparticle samples (10  $\mu$ L) were dried on to aluminium stubs and coated with platinum [77-79].

## 2.9 Encapsulation efficiency and drug release study

The nanosuspension was centrifuged at 18200 rpm for 15 minutes (Eppendorf 5702 Centrifuge, Beckman Coulter, Hauppauge, NY, USA), followed by withdrawal of supernatants. The encapsulation efficiency of insulin-loaded CS-Dz13Scr nanoparticles was determined using the developed RP-HPLC protocol (section 2.2). Insulin release from CS-Dz13Scr nanoparticles was examined in simulated gastric fluid (hydrochloric acid; pH 2) and simulated intestinal fluid (phosphate buffer; pH 6.8) [11,72,80] by using an orbital shaker (PSU-20i, Biosan, Riga, Latvia; 100 rpm;  $37 \pm 0.5$  °C) at concentrations of 12.31  $\mu$ g/mL. Aliquot (55  $\mu$ L) was withdrawn at 0.5 hr, 1 hr, 2 hr, 3 hr, 4 hr, 5 hr, 6 hr, 8 hr and 10 hr. After ultracentrifugation, 50  $\mu$ L of sample was injected into RP-HPLC and the insulin release profile was determined [67].

## 2.10 Cell culture

HT29 cells (human epithelial colorectal adenocarcinoma cells) at passage number of 8-11 and C2C12 cells (mouse myoblasts) at passage number of 10-13 were provided from the American Type Culture Collection (USA). The cells were cultured on T-75 flasks at 37 °C and incubated in a humidified CO<sub>2</sub>CELL 170 incubator (MMM, Germany) containing 5% CO<sub>2</sub> and 95% air. The cell culture medium contained Dulbecco's Modified Eagle Medium, supplemented with fetal bovine serum (10% v/v), sodium bicarbonate (1.5 g/L), and penicillin-streptomycin (100 U/mL, 1% v/v) [81,82]. The cell culture medium was changed every second day.

## 2.11 Cytotoxicity

The cytotoxicity of insulin-loaded nanoparticles was assessed by HT29 cells and C2C12 cells by using Cell-Titre Blue assay (Promega, NSW, Australia). The HT29 cells were seeded in 96-well culture plates (Nunc, Denmark) at  $1 \times 10^5$  cells/well until the formation of cell monolayer [83]. In Dulbecco's Modified Eagle Medium (without FBS), the HT29 cells were treated with blank medium

(negative control), free insulin (100 µg/mL), Dz13Scr (10 µg), chitosan (0.004%) and insulin-loaded nanoparticles (containing 100 µg/mL insulin) for 24 hours. Also, the C2C12 cells were seeded in 96-well cell culture plate at  $1 \times 10^5$  cells/well for 24 h to ascertain cell attachment [84]. The C2C12 cells were exposed to the blank medium (negative control), free insulin (100 nM), Dz13Scr (10 µg), chitosan (0.004%) and insulin-loaded nanoparticles (containing 100 nM insulin) for 24 hours. After sample treatment, the cells were washed with phosphate buffer saline. The cytotoxicity assay was conducted by the established protocol from manufacturer. The cell viability was presented in percentage in relative to non-treated cells.

### **3. Results and discussion**

In the present study, the nanoparticles were prepared by complex coacervation to achieve the essential information. The independent linear effects and interaction effects of 2 manipulated parameters on the dependent responses (particle size, zeta potential and polydispersity index) were acquired. In food science and pharmaceutical research, polynomial equations and RSM plots have been widely employed to evaluate the outcomes of interest. In terms of drug delivery, small and uniform particles with appropriate surface charge and drug release characteristic are ideal to enhance drug retention and absorption in GI tract.

#### **3.1 Preparation of insulin-loaded nanoparticles**

Nanoparticles produced by a mild coacervation method would be ideal for peptides, cells and genes encapsulation. Complex coacervation can lead to spontaneous formation of nanoparticles by oppositely charged molecules [53]. In this study, high temperature, sonication or harmful chemicals were not involved in the preparation of nanoparticles. This technique is simple and mild, thereby the conformational structure and bioactivity of peptides can be preserved by gentle encapsulation conditions. Chitosan concentrations ranging from 0.00004% to 0.25% and Dz13Scr amount ranging from 5 µg to 15 µg were adopted to optimise the insulin formulations (**Table 2**).

#### **3.2 Experimental conditions for the preparation of insulin-loaded nanoparticles**

When compared to insulin (58 kDa), bovine serum albumin (66.5 kDa) possesses comparable molecular weight and physicochemical properties. Due to its relatively low cost, bovine serum albumin has been employed extensively as a model protein in drug development [14,85-87]. In the

preliminary study, bovine serum albumin was used as a model drug to prepare nanoparticles due to its relatively low cost as compared to insulin. In the preliminary study, when bovine serum albumin was used as a model drug to prepare nanoparticles, we observed that preparation time, stirring speed and microfuge tube size had significant effects on the size, polydispersity index and zeta potential of bovine serum albumin-loaded particles (i.e. **data not shown**). In brief, the use of a large microfuge tube (1500  $\mu$ L) was less preferable than small microfuge tube (600  $\mu$ L) due to the production of large unloaded nanoparticles ( $> 770$  nm). It is hypothesized that small-sized microfuge tube had a larger surface area to volume ratio for the pharmaceutical excipients to interact, which facilitate the formation and complexation of nanoparticles with narrower size distribution. Therefore, small-sized microfuge tube (600  $\mu$ L) is recommended for protein encapsulation. In terms of preparation time, sufficient time is essential for the reaction of excipients and fabrication of nanoparticles [88]. In the preliminary study, a reduction in preparation time from 30 seconds to 15 seconds could negatively impact the size ( $> 800$  nm) and polydispersity index ( $> 0.427$ ) of bovine serum albumin-loaded nanoparticles. Last but not least, bovine serum albumin-loaded nanoparticles (prepared by low vortexing speed; 20 Hertz) also demonstrated a significantly higher mean particle size than the formulation that was prepared by the speed at 40 Hertz in the preliminary study. Similarly, previous studies also reported that a higher stirring rate could accelerate the dispersion of the excipients and reduce particle size of chitosan nanoparticles [89] and polylactic acid nanoparticles [90]. Therefore, in the current study, small-sized microfuge tube size (600  $\mu$ L), preparation time (30 second) and speed (40 Hertz) were applied to prepare the insulin-loaded nanoparticles.

### 3.3 Physicochemical properties of insulin-loaded nanoparticles

Oral bioavailability of proteins is normally low due to its instability in GI tract, mucus turnover and poor absorption in the intestine [91-93]. Therefore, the physical characteristics of particles are crucial for efficient peptide absorption in the GI tract. The particle size, polydispersity index and zeta potential of insulin-loaded particles were illustrated in **figure 2**. By adjusting the combination of chitosan concentration and Dz13Scr concentration, both insulin-loaded CS-Dz13Scr nanoparticles and insulin-loaded CS-Dz13Scr microparticles could be generated with various physical characteristics. Overall, the best insulin-loaded CS-Dz13Scr nanoparticles formulation, consisting of 0.004% chitosan and 10  $\mu$ g Dz13Scr, demonstrated the smallest particle size (159.3 nm) and a reasonable polydispersity index (0.331) (**Table 2**). The zeta potential of the best formulation was slightly negative (-1.08 mV). The particle size is deemed to be one of the main physicochemical features of the nanoparticles. It was reported that the permeability of the

nanoparticles across the GI tract increased as the particle size decreased [8,94]. The samples consisting of 0.0025% and 10  $\mu$ g Dz13Scr would be considered as the second-best formulation. This formulation produced a larger particle size (234.6 nm), but the polydispersity index (0.283) and zeta potential (-0.56 mV) were both similar to the best formulation. Surface charge of the drug delivery systems is directly related to the excipients' ratio. The zeta potential of insulin-loaded CS-Dz13Scr nanoparticles tended to be negatively-charged for formulations with low chitosan concentration (0.00004% to 0.025%), or formulations containing high amount of Dz13Scr and 0.04% chitosan. In contrast, the zeta potential of particles became positive when a higher concentration of chitosan (0.25%) solution was added. Thus, one can deduce that the zeta potential is influenced by the presence of excess chitosan on the CS-Dz13Scr particle surface.

### 3.4 Statistical evaluation of the physicochemical characteristics of insulin-loaded nanoparticles

Independent variables, including polymer concentration and oligonucleotide concentration, can interact to produce the dependent effects of nanoparticulate formulations. Previous studies demonstrated that the concentration of excipients (e.g. poly(hydroxybutyrate-co-hydroxyvalerate) [52], polyvinyl alcohol [52]) could have critical effect on the physicochemical properties of nanoparticles. To explore and understand the main independent effects and interaction effects of chitosan concentration and Dz13Scr concentration, the non-linear quadratic statistical model was formulated to elucidate the effect of the independent variables and their interactions on formation of insulin-loaded CS-Dz13Scr particles. Insulin-loaded CS-Dz13Scr particles were evaluated statistically by the polynomial equations that were generated by using Analysis of Variance. The generated quadratic model was found to be useful in predicting size ( $F = 5.33$ ;  $p\text{-value} = 0.0035$ ) and zeta potential ( $F = 5.19$ ;  $p\text{-value} = 0.004$ ). According to the largest absolute value of coefficients in **equation 1, 2 and 3**, chitosan concentration was the most influential factor associated with size, polydispersity index and zeta potential (**Table 3**). Results from ANOVA showed that only the chitosan concentration was significant ( $p < 0.0001$ ) in predicting the size of insulin-loaded CS-Dz13Scr particles. On the other hand, both chitosan concentration ( $p = 0.0059$ ) and squared term of chitosan ( $p = 0.0017$ ) were significant factors that affect the surface charge of particles (**Table 3**). This phenomenon can be attributed to the availability of positively-charged amino groups during interaction with negatively-charged Dz13Scr. The interaction coefficient between chitosan concentration and Dz13Scr amount was not significant in predicting size, polydispersity index and zeta potential. **Figure 3** illustrates the response surface plots for insulin-loaded CS-Dz13Scr particles by setting 100 nM insulin as a fixed constraint. **Table 3** outlines the main effect,

significant coefficients, impact of main and interaction parameters on the outcome responses (size, polydispersity index, zeta potential) for insulin-loaded CS-Dz13Scr particles.

$$\text{Size} =$$

$$7019.1 + 135.91X_1 - 5.41X_2 + 27.17X_1X_2 - 6137.79X_1^2 - 539.55X_2^2 \text{ (equation 1)}$$

$$\text{Polydispersity index} = 0.53 - 0.046X_1 + 0.03X_2 + 0.022X_1X_2 - 7.142E^{-003}X_1^2 + 1.542E^{-003}X_2^2 \text{ (equation 2)}$$

$$\text{Zeta potential} =$$

$$-18.28 + 5.68X_1 - 0.81X_2 + 0.38X_1X_2 + 22.42X_1^2 - 0.23X_2^2 \text{ (equation 3),}$$

where  $X_1$  and  $X_2$  denote chitosan concentration and Dz13Scr amount.

### 3.5 Stability of the physicochemical properties

The stability of the physicochemical properties of the nanoparticles can influence the cellular interaction, GI absorption efficiency, mucus permeation and therapeutic effect of the formulation [95]. Therefore, the stability of the physicochemical properties has been examined extensively in insulin-loaded nanoparticles [96,97]. For instance, the particle size of insulin-loaded polyvinyl alcohol-coated nanoparticles could be maintained when the formulation was being stored for 21 days at 4 °C [98], while the particle size of insulin-loaded hyaluronic acid-coated nanoparticles could be conserved for at least 1 month under both 4 and 25 °C. In **Figure 4(a)**, **Figure 4(b)** and **Figure 4(c)**, the particle size, polydispersity index and zeta potential stability of the developed insulin-loaded nanoparticles were presented respectively. As compared to the freshly prepared formulation, statistical analysis revealed that the developed insulin-loaded nanoparticles did not present any significant difference in particle size (172.73 nm;  $p > 0.05$ ), polydispersity index (0.34;  $p > 0.05$ ) and zeta potential (-1.27 mV;  $p > 0.05$ ). Therefore, the nanoparticles that were prepared by chitosan and Dz13Scr could maintain the stability of the formulation, and the physiochemical properties of nanoparticles were preserved upon storage.

### 3.6 FTIR-ATR examination of insulin-loaded nanoparticles

The functional groups of insulin-loaded CS-Dz13Scr nanoparticles were examined by FTIR-ATR spectroscopy. **Figure 4(d)** illustrates the FTIR spectra of 100 nM insulin, freshly prepared 100 nM of insulin-loaded CS-Dz13Scr nanoparticles and insulin-loaded CS-Dz13Scr nanoparticles (1-month storage). In the 100 nM insulin FTIR spectra, the characteristic peaks were obtained at 1643

cm<sup>-1</sup> (-C=O stretching) and 1558 cm<sup>-1</sup> (N-H bending) for amide I band and amide II band respectively. The formation of insulin-loaded CS-Dz13Scr nanoparticles was confirmed, which demonstrated similar peak at 1642-1644 cm<sup>-1</sup> and 1558 cm<sup>-1</sup>. The FTIR analysis revealed that complex coacervation had no negative impact on the stability and characteristic amide bands of insulin. Upon storage of the formulation for 1-month, the stability of the insulin-loaded nanoparticles was maintained as shown by the FTIR spectra.

### 3.6 Encapsulation efficiency and drug release analysis of insulin-loaded nanoparticles

In the present study, RP-HPLC was utilized to quantify the encapsulation efficiency of the insulin-loaded CS-Dz13Scr nanoparticles. The RP-HPLC calibration showed good linearity for 8 standard solution (2.9 to 202 µg/mL) with R<sup>2</sup> greater than 0.998. The encapsulation efficiency of the formulation was 70.72 ± 0.23 %. In **Figure 5**, insulin-loaded CS-Dz13Scr nanoparticles demonstrated a burst release profile in both SGF (31.02%) and SIF (27.87%) at 37 °C within 30 minutes. It indicated that insulin desorption occurred at the surface of the nanoparticles. After initial rapid release, all encapsulated insulin was released at a controlled pattern over 10 hours in SGF due to the diffusion of the encapsulated drug from the core of nanoparticles, whereas the percentage of insulin released was 91.73% over 10 hours in SIF. The obtained data demonstrated that RP-HPLC could analyse the encapsulation efficiency and amount of insulin release from polymeric-oligonucleotide formulations.

### 3.7 Cytotoxic effect of insulin-loaded nanoparticles

Previous studies showed that polymeric nanoparticle presented satisfactory safety profile and negligible toxicity [8,53,99,100]. For instance, the lyophilized insulin-loaded modified chitosan nanoparticles did not show any toxicity in GI cells after being treated for 3 h [8]. For the pharmaceutical development of insulin-loaded nanoparticles, HT29 cells [101] and C2C12 cells [102,103] have been used extensively as the *in vitro* intestinal model and *in vitro* insulin-responsive skeletal muscle cell model respectively. In the current study, as shown in **Figure 6(a)**, all tested samples displayed at least 94% of HT29 cell viability. Statistical analysis by Analysis of Variance showed that insulin, Dz13Scr, chitosan and insulin-loaded nanoparticles had no significant difference in mean cell viabilities as compared to non-treated cells (negative control) ( $p > 0.05$ ). When C2C12 cells were exposed to insulin, Dz13Scr, chitosan and insulin-loaded nanoparticles, the samples did not elicit any cytotoxicity to the C2C12 cells. As shown in **Figure 6(b)**, the C2C12 cell viability was at least 90% after being incubated with the samples. When compared to the negative



control, Analysis of Variance revealed that all tested samples introduced negligible cytotoxicity to the C2C12 cells. Therefore, the fabricated nanoparticles and excipients in the formulation were biocompatible and safe at the tested concentration.

### 3.8 Potential applications of insulin-loaded nanoparticles

Nanoparticle is a promising drug delivery system that can enhance the stability and absorption of instable therapeutic agents by withstanding drug degradation, promoting GI adhesion and demonstrating controlled drug release behaviour. In this study, the insulin-loaded nanoparticles were loaded in the nanoparticles by complex coacervation technique using Dz13Scr and biodegradable chitosan with promising size and zeta potential. As shown in **Figure 5**, the spherical nanoparticles were generated in this technique. As compared to dynamic light scattering, the obtained particle size in scanning electron microscopy was smaller. Previous literature stated that the phenomenon was attributed to the removal of water molecules from the samples, which nullified the effect of sample swelling [97,104,105]. Insulin is an amphoteric molecule that can be encapsulated into the particles that are composed of chitosan and Dz13Scr. Its chemical interaction with polymers includes ionic, hydrogen and van der Waal's forces. The positively-charged chitosan can form complexes with negatively-charged residues of Dz13Scr and insulin. In the GI tract, the mucoadhesiveness of chitosan-based formulation could enhance the stability and absorption of therapeutic peptides [106]. We reported that 0.004% chitosan and 10 µg Dz13Scr could generate a successful insulin-loaded CS-Dz13Scr nanoparticulate formulation with the smallest particle size (159.3 nm) and a reasonable polydispersity index (0.331). Previous studies demonstrated that particles with small size was favourable for the mucosal diffusion and GI absorption of insulin-loaded nanoparticles [8,107,108].

This study revealed the potential of CS-Dz13Scr nanoparticulate system for oral delivery of insulin. Insulin is a protein with 51 amino acids commonly injected subcutaneously in the management of diabetes mellitus. Although various strategies have been investigated to enhance the oral bioavailability of peptides [91], nanoparticulate drug delivery systems remain the most attractive approach, due to its capacity in shielding the encapsulated therapeutic agents, and promoting drug absorption by both paracellular and transcellular routes [10]. However, burst release of insulin was observed in the drug release study for the developed formulation. The following strategies, including the use of enteric-coated polymeric coatings (e.g. Eudragit® FS 30D [109], hydroxypropyl methylcellulose phthalate [110]), modified natural polymers (e.g. methylated chitosan [55]), enteric-coated tablets, and enteric-coated capsules [110], are warranted in future

studies. These strategies have been proven to minimise the wastage of costly protein and mitigate the effect of burst release. Furthermore, the immunogenicity, biocompatibility and pharmacokinetic response of the orally administered formulation should be examined in future studies. Apart from blood sugar level management, insulin-loaded CS-Dz13Scr nanoparticles can be potentially applied to promote tissue healing [111] in patients with chronic wounds and diabetic ulcers, which reduced wound healing time when incorporated into topical cream [112] and spray-based formulation [113]. Last but not least, insulin-loaded CS-Dz13Scr nanoparticles can be a potential drug delivery system to induce bone cell proliferation [114], osteoblast differentiation [115] and bone mineralization [116,117]. Insulin is also a hormone involving in bone energy metabolism and bone remodelling [118,119]. Its potential in diabetes treatment, wound healing and bone cells proliferation should be investigated.

#### **4. Conclusion**

In the present study, insulin-loaded CS-Dz13Scr nanoparticles were successfully prepared by complex coacervation. Through the self-assembling process, nanoparticles could be prepared in an absence of harsh chemical. The formulation was characterized in terms of particle size, polydispersity index and zeta potential. The physical characteristics and drug release profile of particles are crucial for stability, mucosal adhesion and efficient absorption. This study examined the effect of 2 factors, including polymer concentration and oligonucleotide concentration, that could influence the physical characteristics of particles. The obtained results revealed satisfactory results for insulin-loaded CS-Dz13Scr nanoparticles (159.3 nm, pdi 0.331, -1.08 mV). The pharmaceutical excipients used in the present study are known to be biodegradable, biocompatible and harmless to GI cells and skeletal muscle cells.

#### **5. Conflict of interest**

The authors declare that they have no conflicts of interest to disclose.

## 6. Acknowledgements

This paper was not prepared with a specific grant from any funding agency in the public, commercial, or not-for-profit sectors. Wong acknowledges the support from Australian Government through Australian Government Research Training Program Scholarship. Al-Salami is partially supported by the European Union's Horizon 2020 SALSETH research and innovation programme under the Marie Skłodowska-Curie grant agreement No 872370.

## Reference

1. Zhang Z, Cai H, Liu Z, et al. Effective enhancement of hypoglycemic effect of insulin by liver-targeted nanoparticles containing cholic acid-modified chitosan derivative. *Mol Pharmaceut.* 2016;13(7):2433-2442.
2. Bai X, Kong M, Xia G, et al. Systematic investigation of fabrication conditions of nanocarrier based on carboxymethyl chitosan for sustained release of insulin. *Int J Biol Macromol.* 2017;102:468-474.
3. Chopra S, Bertrand N, Lim JM, et al. Design of insulin-loaded nanoparticles enabled by multistep control of nanoprecipitation and zinc chelation. *Acs Appl Mater Inter.* 2017;9(13):11440-11450.
4. Pereira de Sousa I, Moser T, Steiner C, et al. Insulin loaded mucus permeating nanoparticles: Addressing the surface characteristics as feature to improve mucus permeation. *Int J Pharm.* 2016;500(1-2):236-244.
5. Wong CY, Al-Salami H, Dass CR. Microparticles, microcapsules and microspheres: A review of recent developments and prospects for oral delivery of insulin. *Int J Pharm.* 2018;537(1-2):223-244.
6. Fasano A. Innovative strategies for the oral delivery of drugs and peptides. *Trends Biotechnol.* 1998;16(4):152-157.
7. Lee VHL, Yamamoto A. Penetration and enzymatic barriers to peptide and protein absorption. *Adv Drug Deliv Rev.* 1989;4(2):171-207.
8. Mahjub R, Radmehr M, Dorkoosh FA, et al. Lyophilized insulin nanoparticles prepared from quaternized n-aryl derivatives of chitosan as a new strategy for oral delivery of insulin: In vitro, ex vivo and in vivo characterizations. *Drug Dev Ind Pharm.* 2014;40(12):1645-1659.
9. Sonaje K, Lin YH, Juang JH, et al. In vivo evaluation of safety and efficacy of self-assembled nanoparticles for oral insulin delivery. *Biomaterials.* 2009;30(12):2329-2339.

10. Wong CY, Al-Salami H, Dass CR. Potential of insulin nanoparticle formulations for oral delivery and diabetes treatment. *J Control Release*. 2017;264:247-275.
11. Salvioni L, Fiandra L, Del Curto MD, et al. Oral delivery of insulin via polyethylene imine-based nanoparticles for colonic release allows glycemic control in diabetic rats. *Pharmacol Res*. 2016;110:122-130.
12. Avadi MR, Sadeghi AMM, Mohamadpour Dounighi N, et al. Ex vivo evaluation of insulin nanoparticles using chitosan and arabic gum. *ISRN Pharm*. 2011;2011:860109.
13. Ilium L. Chitosan and its use as a pharmaceutical excipient. *Pharm Res*. 1998;15(9):1326-1331.
14. Yin L, Wang Y, Wang C, et al. Nano-reservoir bioadhesive tablets enhance protein drug permeability across the small intestine. *AAPS PharmSciTech*. 2017;18(6):2329-2335.
15. Chen JX, Liu C, Shan W, et al. Enhanced stability of oral insulin in targeted peptide ligand trimethyl chitosan nanoparticles against trypsin. *J Microencapsul*. 2015;32(7):632-641.
16. Steichen S, O'Connor C, Peppas NA. Development of a p((maa-co-nvp)-g-eg) hydrogel platform for oral protein delivery: effects of hydrogel composition on environmental response and protein partitioning. *Macromol Biosci*. 2017;17(1):1-15.
17. Barbari GR, Dorkoosh FA, Amini M, et al. A novel nanoemulsion-based method to produce ultrasmall, water-dispersible nanoparticles from chitosan, surface modified with cell-penetrating peptide for oral delivery of proteins and peptides. *Int J Nanomedicine*. 2017;12:3471-3483.
18. Rishi P, Bhogal A, Arora S, et al. Improved oral therapeutic potential of nanoencapsulated cryptdin formulation against salmonella infection. *Eur J Pharm Sci*. 2015;72:27-33.
19. Kanwar JR, Mahidhara G, Kanwar RK. Novel alginate-enclosed chitosan-calcium phosphate-loaded iron-saturated bovine lactoferrin nanocarriers for oral delivery in colon cancer therapy. *Nanomedicine*. 2012;7(10):1521-1550.
20. Samarasinghe RM, Kanwar RK, Kanwar JR. The effect of oral administration of iron saturated-bovine lactoferrin encapsulated chitosan-nanocarriers on osteoarthritis. *Biomaterials*. 2014;35(26):7522-7534.
21. Kanwar JR, Mahidhara G, Roy K, et al. Fe-blf nanoformulation targets survivin to kill colon cancer stem cells and maintains absorption of iron, calcium and zinc. *Nanomedicine*. 2015;10(1):35-55.
22. Mahidhara G, Kanwar RK, Roy K, et al. Oral administration of iron-saturated bovine lactoferrin-loaded ceramic nanocapsules for breast cancer therapy and influence on iron and calcium metabolism. *Int J Nanomedicine*. 2015;10:4081-4098.

23. Anand N, Sehgal R, Kanwar RK, et al. Oral administration of encapsulated bovine lactoferrin protein nanocapsules against intracellular parasite toxoplasma gondii. *Int J Nanomedicine*. 2015;10:6355-6369.
24. Ribeiro C, Neto AP, das Neves J, et al. Preparation of polyelectrolyte nanocomplexes containing recombinant human hepatocyte growth factor as potential oral carriers for liver regeneration. *Methods Mol Biol*. 2012;811:113-125.
25. Su FY, Chuang EY, Lin PY, et al. Treatment of chemotherapy-induced neutropenia in a rat model by using multiple daily doses of oral administration of g-csf-containing nanoparticles. *Biomaterials*. 2014;35(11):3641-3649.
26. Qi LF, Xu ZR, Li Y, et al. In vitro effects of chitosan nanoparticles on proliferation of human gastric carcinoma cell line mgc803 cells. *World J Gastroenterol*. 2005;11(33):5136-5141.
27. Aliasghari A, Rabbani Khorasgani M, Vaezifar S, et al. Evaluation of antibacterial efficiency of chitosan and chitosan nanoparticles on cariogenic streptococci: an in vitro study. *Iran J Microbiol*. 2016;8(2):93-100.
28. Li X, Min M, Du N, et al. Chitin, chitosan, and glycated chitosan regulate immune responses: The novel adjuvants for cancer vaccine. *Clin Dev Immunol*. 2013;2013:387023.
29. Wong CY, Al-Salami H, Dass CR. Recent advancements in oral administration of insulin-loaded liposomal drug delivery systems for diabetes mellitus. *Int J Pharm*. 2018;549(1-2):201-217.
30. Vivek R, Nipun Babu V, Thangam R, et al. Ph-responsive drug delivery of chitosan nanoparticles as tamoxifen carriers for effective anti-tumor activity in breast cancer cells. *Colloids Surf B Biointerfaces*. 2013;111:117-123.
31. Chuang EY, Lin KJ, Su FY, et al. Noninvasive imaging oral absorption of insulin delivered by nanoparticles and its stimulated glucose utilization in controlling postprandial hyperglycemia during oggtt in diabetic rats. *J Control Release*. 2013;172(2):513-522.
32. Zhi J, Wang Y, Luo G. Adsorption of diuretic furosemide onto chitosan nanoparticles prepared with a water-in-oil nanoemulsion system. *React Funct Polym*. 2005;65(3):249-257.
33. Nishimura K, Nishimura S, Nishi N, et al. Immunological activity of chitin and its derivatives. *Vaccine*. 1984;2(1):93-99.
34. Nishimura K, Ishihara C, Ukei S, et al. Stimulation of cytokine production in mice using deacetylated chitin. *Vaccine*. 1986;4(3):151-156.
35. Da Silva CA, Pochard P, Lee CG, et al. Chitin particles are multifaceted immune adjuvants. *American journal of respiratory and critical care medicine*. 2010;182(12):1482-1491.
36. Nishimura K, Nishimura S, Nishi N, et al. Adjuvant activity of chitin derivatives in mice and guinea-pigs. *Vaccine*. 1985;3(5):379-384.

37. Wen ZS, Xu YL, Zou XT, et al. Chitosan nanoparticles act as an adjuvant to promote both th1 and th2 immune responses induced by ovalbumin in mice. *Mar Drugs*. 2011;9(6):1038-1055.
38. Wu KY, Wu M, Fu ML, et al. A novel chitosan cpg nanoparticle regulates cellular and humoral immunity of mice. *Biomed Environ Sci*. 2006;19(2):87-95.
39. Yousefpour P, Atyabi F, Vasheghani-Farahani E, et al. Targeted delivery of doxorubicin-utilizing chitosan nanoparticles surface-functionalized with anti-her2 trastuzumab. *Int J Nanomedicine*. 2011;6:1977-1990.
40. Elahy M, Dass CR. Dz13: C-jun downregulation and tumour cell death. *Chem Biol Drug Des*. 2011;78(6):909-912.
41. Chan CWS, Kaplan W, Parish CR, et al. Reduced retinal microvascular density, improved forepaw reach, comparative microarray and gene set enrichment analysis with c-jun targeting DNA enzyme. *Plos One*. 2012;7(7):e39160.
42. Santiago FS, Lowe HC, Kavurma MM, et al. New DNA enzyme targeting egr-1 mrna inhibits vascular smooth muscle proliferation and regrowth after injury. *Nat Med*. 1999;5(12):1264-1269.
43. Tan ML, Dunstan DE, Friedhuber AM, et al. A nanoparticulate system that enhances the efficacy of the tumoricide dz13 when administered proximal to the lesion site. *J Control Release*. 2010;144(2):196-202.
44. Tan ML, Friedhuber AM, Dass CR. Co-nanoencapsulated doxorubicin and dz13 control osteosarcoma progression in a murine model. *J Pharm Pharmacol*. 2013;65(1):35-43.
45. Fokina AA, Stetsenko DA, François JC. DNA enzymes as potential therapeutics: towards clinical application of 10-23 dnazymes. *Expert Opin Biol Ther*. 2015;15(5):689-711.
46. Cai H, Santiago FS, Prado-Lourenco L, et al. DNAzyme targeting c-jun suppresses skin cancer growth. *Sci Transl Med*. 2012;4(139):139ra82.
47. Dicke T, Pali-Schöll I, Kaufmann A, et al. Absence of unspecific innate immune cell activation by gata-3-specific dnazymes. *Nucleic Acid Ther*. 2012;22(2):117-126.
48. Fuhst R, Runge F, Buschmann J, et al. Toxicity profile of the gata-3-specific dnzyme hgd40 after inhalation exposure. *Pulm Pharmacol Ther*. 2013;26(2):281-289.
49. Cho EA, Moloney FJ, Cai H, et al. Safety and tolerability of an intratumorally injected dnzyme, dz13, in patients with nodular basal-cell carcinoma: A phase 1 first-in-human trial (discover). *Lancet*. 2013;381(9880):1835-1843.
50. Sparreboom A, Scripture CD, Trieu V, et al. Comparative preclinical and clinical pharmacokinetics of a cremophor-free, nanoparticle albumin-bound paclitaxel (abi-007) and paclitaxel formulated in cremophor (taxol). *Clin Cancer Res*. 2005;11(11):4136-4143.

51. Reinholz J, Landfester K, Mailänder V. The challenges of oral drug delivery via nanocarriers. *Drug Deliv*. 2018;25(1):1694-1705.
52. Bayrami S, Esmaili Z, SeyedAlinaghi S, et al. Fabrication of long-acting insulin formulation based on poly (3-hydroxybutyrate-co-3-hydroxyvalerate) (phbv) nanoparticles: Preparation, optimization, characterization, and in-vitro evaluation. *Pharm Dev Technol*. 2019;24(2):176-188.
53. Shamsa ES, Mahjub R, Mansoorpour M, et al. Nanoparticles prepared from n,n-dimethyl-n-octyl chitosan as the novel approach for oral delivery of insulin: Preparation, statistical optimization and in-vitro characterization. *Iran J Pharm Res*. 2018;17(2):442-459.
54. Avadi MR, Sadeghi AM, Mohammadpour N, et al. Preparation and characterization of insulin nanoparticles using chitosan and arabic gum with ionic gelation method. *Nanomedicine*. 2010;6(1):58-63.
55. Mahjub R, Dorkoosh FA, Amini M, et al. Preparation, statistical optimization, and in vitro characterization of insulin nanoparticles composed of quaternized aromatic derivatives of chitosan. *AAPS PharmSciTech*. 2011;12(4):1407-1419.
56. Woitiski CB, Veiga F, Ribeiro A, et al. Design for optimization of nanoparticles integrating biomaterials for orally dosed insulin. *Eur J Pharm Biopharm*. 2009;73(1):25-33.
57. Attivi D, Wehrle P, Ubrich N, et al. Formulation of insulin-loaded polymeric nanoparticles using response surface methodology. *Drug Dev Ind Pharm*. 2005;31(2):179-189.
58. Sarmiento B, Martins S, Ferreira D, et al. Oral insulin delivery by means of solid lipid nanoparticles. *Int J Nanomed*. 2007;2(4):743-749.
59. Pridgen EM, Alexis F, Kuo TT, et al. Transepithelial transport of fc-targeted nanoparticles by the neonatal fc receptor for oral delivery. *Sci Transl Med*. 2013;5(213):213ra167.
60. Jafary Omid N, Morovati H, Amini M, et al. Development of molecularly imprinted olanzapine nano-particles: In vitro characterization and in vivo evaluation. *AAPS PharmSciTech*. 2016;17(6):1457-1467.
61. Gupta B, Poudel BK, Pathak S, et al. Effects of formulation variables on the particle size and drug encapsulation of imatinib-loaded solid lipid nanoparticles. *AAPS PharmSciTech*. 2016;17(3):652-662.
62. Turk CT, Oz UC, Serim TM, et al. Formulation and optimization of nonionic surfactants emulsified nimesulide-loaded plga-based nanoparticles by design of experiments. *AAPS PharmSciTech*. 2014;15(1):161-176.
63. Reis CP, Ribeiro AJ, Veiga F, et al. Polyelectrolyte biomaterial interactions provide nanoparticulate carrier for oral insulin delivery. *Drug Deliv*. 2008;15(2):127-139.
64. Gupta R, Mohanty S. Controlled release of insulin from folic acid-insulin complex nanoparticles. *Colloids Surf B Biointerfaces*. 2017;154:48-54.

65. Liu C, Kou Y, Zhang X, et al. Enhanced oral insulin delivery via surface hydrophilic modification of chitosan copolymer based self-assembly polyelectrolyte nanocomplex. *Int J Pharma*. 2019;554:36-47.
66. Ibie CO, Knott RM, Thompson CJ. Complexation of novel thiomers and insulin to protect against in vitro enzymatic degradation - towards oral insulin delivery. *Drug Dev Ind Pharm*. 2019;45(1):67-75.
67. Wong CY, Martinez J, Al-Salami H, et al. Quantification of bsa-loaded chitosan/oligonucleotide nanoparticles using reverse-phase high-performance liquid chromatography. *Anal Bioanal Chem*. 2018;410(27):6991-7006.
68. Hosseini-Nassab N, Samanta D, Abdolazimi Y, et al. Electrically controlled release of insulin using polypyrrole nanoparticles. *Nanoscale*. 2017;9(1):143-149.
69. Rho JG, Han HS, Han JH, et al. Self-assembled hyaluronic acid nanoparticles: Implications as a nanomedicine for treatment of type 2 diabetes. *J Control Release*. 2018;279:89-98.
70. Cui Y, Shan W, Zhou R, et al. The combination of endolysosomal escape and basolateral stimulation to overcome the difficulties of "easy uptake hard transcytosis" of ligand-modified nanoparticles in oral drug delivery. *Nanoscale*. 2018;10(3):1494-1507.
71. Yang L, Li M, Sun Y, et al. A cell-penetrating peptide conjugated carboxymethyl- $\beta$ -cyclodextrin to improve intestinal absorption of insulin. *Int J Biol Macromol*. 2018;111:685-695.
72. Prusty Ak, Sahu SK. Development and evaluation of insulin incorporated nanoparticles for oral administration. *ISRN Nanotechnology*. 2013;2013:1-6.
73. Woitiski CB, Neufeld RJ, Ribeiro AJ, et al. Colloidal carrier integrating biomaterials for oral insulin delivery: influence of component formulation on physicochemical and biological parameters. *Acta Biomater*. 2009;5(7):2475-2484.
74. Sarmiento B, Ribeiro A, Veiga F, et al. Development and characterization of new insulin containing polysaccharide nanoparticles. *Colloids Surf B Biointerfaces*. 2006;53(2):193-202.
75. Sarmiento B, Martins S, Ribeiro A, et al. Development and comparison of different nanoparticulate polyelectrolyte complexes as insulin carriers. *Int J Pept Res Ther*. 2006;12(2):131-138.
76. Sarmiento B, Ferreira D, Veiga F, et al. Characterization of insulin-loaded alginate nanoparticles produced by ionotropic pre-gelation through dsc and ftir studies. *Carbohydr Polym*. 2006;66(1):1-7.
77. Siddiqui NA, Billa N, Roberts CJ. Multiboronic acid-conjugated chitosan scaffolds with glucose selectivity to insulin release. *J Biomater Sci Polym Ed*. 2017;28(8):781-793.



78. Lopes MA, Abraham-Vieira B, Oliveira C, et al. Probing insulin bioactivity in oral nanoparticles produced by ultrasonication-assisted emulsification/internal gelation. *Int J Nanomedicine*. 2015;10:5865-80.
79. Ma Z, Yeoh HH, Lim LY. Formulation pH modulates the interaction of insulin with chitosan nanoparticles. *J Pharm Sci*. 2002;91(6):1396-404.
80. Sgorla D, Lechanteur A, Almeida A, et al. Development and characterization of lipid-polymeric nanoparticles for oral insulin delivery. *Expert Opin Drug Deliv*. 2018;15(3):213-222.
81. Wong CY, Al-Salami H, Dass CR. Cellular assays and applied technologies for characterisation of orally administered protein nanoparticles: A systematic review. *J Drug Target*. 2020:1-15.
82. Wong CY, Martinez J, Carnagarin R, et al. In-vitro evaluation of enteric coated insulin tablets containing absorption enhancer and enzyme inhibitor. *J Pharm Pharmacol*. 2017;69(3):285-294.
83. Wong CY, Al-Salami H, Dass CR. Formulation and characterisation of insulin-loaded chitosan nanoparticles capable of inducing glucose uptake in skeletal muscle cells in vitro. *J Drug Deliv Sci Technol*. 2020;57:101738.
84. Wong CY, Al-Salami H, Dass CR. Lyophilisation improves bioactivity and stability of insulin-loaded polymeric-oligonucleotide nanoparticles for diabetes treatment. *AAPS PharmSciTech*. 2020;21(3):108.
85. Shastri PN, Ubale RV, D'Souza MJ. Implementation of mixture design for formulation of albumin containing enteric-coated spray-dried microparticles. *Drug Dev Ind Pharm*. 2013;39(2):164-175.
86. Harde H, Agrawal AK, Jain S. Development of stabilized glucomannosylated chitosan nanoparticles using tandem crosslinking method for oral vaccine delivery. *Nanomedicine*. 2014;9(16):2511-2529.
87. Tantisripreecha C, Jaturanpinyo M, Panyarachun B, et al. Development of delayed-release proliposomes tablets for oral protein drug delivery. *Drug Dev Ind Pharm*. 2012;38(6):718-727.
88. Balavandy SK, Shameli K, Biak DRBA, et al. Stirring time effect of silver nanoparticles prepared in glutathione mediated by green method. *Chem Cent J*. 2014;8(1):11.
89. Mudhakir D, Wibisono C, Rachmawati H. Encapsulation of risperidone into chitosan-based nanocarrier via ionic binding interaction. *Procedia Chem*. 2014;13:92-100.
90. Mulia K, Safiera A, Pane I, et al. Effect of high speed homogenizer speed on particle size of polylactic acid. *J Phys Conf Ser*. 2019;1198:062006.
91. Wong CY, Martinez J, Dass CR. Oral delivery of insulin for treatment of diabetes: Status quo, challenges and opportunities. *J Pharm Pharmacol*. 2016;68(9):1093-1108.

92. Wong CY, Al-Salami H, Dass CR. The role of chitosan on oral delivery of peptide-loaded nanoparticle formulation. *J Drug Target*. 2018;26(7):551-562.
93. Wong CY, Al-Salami H, Dass CR. Current status and applications of animal models in pre-clinical development of orally administered insulin-loaded nanoparticles. *J Drug Target*. 2020:1-22.
94. Sankalia MG, Mashru RC, Sankalia JM, et al. Reversed chitosan–alginate polyelectrolyte complex for stability improvement of alpha-amylase: optimization and physicochemical characterization. *Eur J Pharm Biopharm*. 2007;65(2):215-232.
95. Wong CY, Luna G, Martinez J, et al. Bio-nanotechnological advancement of orally administered insulin nanoparticles: Comprehensive review of experimental design for physicochemical characterization. *Int J Pharm*. 2019;572:118720.
96. He Z, Liu Z, Tian H, et al. Scalable production of core-shell nanoparticles by flash nanocomplexation to enhance mucosal transport for oral delivery of insulin. *Nanoscale*. 2018;10(7):3307-3319.
97. Presas E, McCartney F, Sultan E, et al. Physicochemical, pharmacokinetic and pharmacodynamic analyses of amphiphilic cyclodextrin-based nanoparticles designed to enhance intestinal delivery of insulin. *J Control Release*. 2018;286:402-414.
98. Czuba E, Diop M, Mura C, et al. Oral insulin delivery, the challenge to increase insulin bioavailability: Influence of surface charge in nanoparticle system. *Int J Pharm*. 2018;542(1-2):47-55.
99. Tong F, Liu S, Yan B, et al. Endogenous ornithine decarboxylase/polyamine system mediated the antagonist role of insulin/peg-cmcs preconditioning against heart ischemia/reperfusion injury in diabetes mellitus. *Int J Nanomedicine*. 2018;13:2507-2520.
100. Bhattacharyya A, Nasim F, Mishra R, et al. Polyurethane-incorporated chitosan/alginate core-shell nano - particles for controlled oral insulin delivery. *J Appl Polym Sci*. 2018;135(26):46365.
101. Alfatama M, Lim LY, Wong TW. Alginate-c18 conjugate nanoparticles loaded in tripolyphosphate-cross-linked chitosan-oleic acid conjugate-coated calcium alginate beads as oral insulin carrier. *Mol Pharm*. 2018;15(8):3369-3382.
102. Zhao Y, Li N, Li Z, et al. Conditioned medium from contracting skeletal muscle cells reverses insulin resistance and dysfunction of endothelial cells. *Metabolism*. 2018;82:36-46.
103. Ayeleso TB, Ramachela K, Mukwevho E. Aqueous-methanol extracts of orange-fleshed sweet potato (*Ipomoea batatas*) ameliorate oxidative stress and modulate type 2 diabetes associated genes in insulin resistant c2c12 cells. *Molecules*. 2018;23(8): E2058.

104. Dhanasekaran S, Rameshthangam P, Venkatesan S, et al. In vitro and in silico studies of chitin and chitosan based nanocarriers for curcumin and insulin delivery. *J Polym Environ*. 2018;26:4095-4113.
105. Andreani T, de Souza AL, Kiill CP, et al. Preparation and characterization of peg-coated silica nanoparticles for oral insulin delivery. *Int J Pharm*. 2014;473(1-2):627-635.
106. Thanou M, Verhoef JC, Junginger HE. Oral drug absorption enhancement by chitosan and its derivatives. *Adv Drug Deliv Rev*. 2001;52(2):117-126.
107. Hecq J, Siepmann F, Siepmann J, et al. Development and evaluation of chitosan and chitosan derivative nanoparticles containing insulin for oral administration. *Drug Dev Ind Pharm*. 2015;41(12):2037-2044.
108. Desai MP, Labhasetwar V, Amidon GL, et al. Gastrointestinal uptake of biodegradable microparticles: effect of particle size. *Pharm Res*. 1996;13(12):1838-1845.
109. Sun S, Liang N, Yamamoto H, et al. Ph-sensitive poly(lactide-co-glycolide) nanoparticle composite microcapsules for oral delivery of insulin. *Int J Nanomedicine*. 2015;10:3489-3498.
110. Cui FD, Tao AJ, Cun DM, et al. Preparation of insulin loaded plga-hp55 nanoparticles for oral delivery. *J Pharm Scie*. 2007;96(2):421-427.
111. Abdelkader DH, Osman MA, El-Gizawy SA, et al. Effect of poly(ethylene glycol) on insulin stability and cutaneous cell proliferation in vitro following cytoplasmic delivery of insulin-loaded nanoparticulate carriers - a potential topical wound management approach. *Eur J Pharm Sci*. 2018;114:372-384.
112. Lima MHM, Caricilli AM, de Abreu LL, et al. Topical insulin accelerates wound healing in diabetes by enhancing the akt and erk pathways: A double-blind placebo-controlled clinical trial. *Plos One*. 2012;7(5):e36974.
113. Wang E, Zhao M, Forrester JV, et al. Electric fields and map kinase signaling can regulate early wound healing in lens epithelium. *Invest Ophthalmol Vis Sci*. 2003;44(1):244-249.
114. Luginbuehl V, Wenk E, Koch A, et al. Insulin-like growth factor i-releasing alginate-tricalciumphosphate composites for bone regeneration. *Pharm Res*. 2005;22(6):940-950.
115. Zhang W, Shen X, Wan C, et al. Effects of insulin and insulin-like growth factor 1 on osteoblast proliferation and differentiation: differential signalling via akt and erk. *Cell Biochem Funct*. 2012;30(4):297-302.
116. Scudeller LA, Mavropoulos E, Tanaka MN, et al. Effects on insulin adsorption due to zinc and strontium substitution in hydroxyapatite. *Mater Sci Eng C Mater Biol Appl*. 2017;79:802-811.
117. Shyong YJ, Tsai CC, Lin RF, et al. Insulin-loaded hydroxyapatite combined with macrophage activity to deliver insulin for diabetes mellitus. *J Mater Chem B*. 2015;3(11):2331-2340.

118. Ferron M, Wei J, Yoshizawa T, et al. Insulin signaling in osteoblasts integrates bone remodeling and energy metabolism. *Cell*. 2010;142(2):296-308.
119. Capilla E, Teles-Garcia A, Acerete L, et al. Insulin and igf-i effects on the proliferation of an osteoblast primary culture from sea bream (*sparus aurata*). *Gen Comp Endocrinol*. 2011;172(1):107-114.

## **Legends to tables and figures**

**Table 1.** Statistical findings and formulation characteristics of insulin-loaded nanoparticles.

**Table 2.** Mean particle size, polydispersity index and zeta potential of insulin-loaded CS-Dz13Scr nanoparticles/microparticles.

**Table 3.** The main effect, significant coefficients, impact of main and interaction parameters on the outcome responses (size, polydispersity index, zeta potential) for insulin-loaded CS-Dz13Scr particles.

**Figure 1.** Schematic presentation of the preparation and pharmaceutical analysis of insulin-loaded nanoparticle.

**Figure 2.** The particle size, polydispersity index and zeta potential of insulin-loaded particles.

**Figure 3.** The response surface plot of insulin-loaded CS-Dz13Scr particles for size distribution, polydispersity index and zeta potential.

**Figure 4.** The stability of physicochemical properties and FTIR spectra of insulin-loaded nanoparticles.

**Figure 5.** The SEM image and drug release profile of insulin-loaded CS-Dz13Scr nanoparticles.

**Figure 6.** The cell viabilities of HT29 cells and C2C12 cells.

**Table 1.** Statistical findings and formulation characteristics of insulin-loaded nanoparticles.

Formulations	Preparation technique	Optimization method	Summary of statistical findings and formulation characteristics	Reference
Insulin-loaded poly (3-hydroxybutyrate-co-3-hydroxyvalerate) Nanoparticles	Double emulsification solvent evaporation method	Box Behnken design	<ul style="list-style-type: none"> <li>● Poly (3-hydroxybutyrate-co-3-hydroxyvalerate) concentration had significant effect on the particle size and polydispersity index.</li> <li>● An increment in polyvinyl alcohol concentration to the optimum value reduced the particle size, but the size increased when the concentration increased beyond the optimum value due to the formation of large emulsion droplets.</li> <li>● The interaction of poly (3-hydroxybutyrate-co-3-hydroxyvalerate) concentration and polyvinyl alcohol concentration had significant effect on the particle size and polydispersity index.</li> <li>● An increase in poly (3-hydroxybutyrate-co-3-hydroxyvalerate) and polyvinyl alcohol concentration increased the polydispersity index due to the generation of rough dispersion.</li> <li>● FTIR spectra showed that insulin-loaded Nanoparticles possessed comparable characteristic peaks of insulin.</li> </ul>	2018: [52]
Lyophilized insulin-loaded N, N-dimethyl-N-octyl chitosan Nanoparticles	Polyelectrolyte complexation	Box Behnken design	<ul style="list-style-type: none"> <li>● The concentration of N-dimethyl-N-octyl chitosan had significant effect on the particle size and polydispersity index.</li> <li>● An increase in polymer concentration (at acidic pH) could increase the particle size and polydispersity index.</li> <li>● High polymer concentration decreased the polydispersity of the formulation.</li> <li>● The Nanoparticles had no cytotoxicity in GI cells after being treated for 5 h.</li> </ul>	2018: [53]
Lyophilized insulin-loaded modified chitosan Nanoparticles	Polyelectrolyte complexation	D-optimal response surface methodology	<ul style="list-style-type: none"> <li>● High level of burst release at alkaline pH with more than 40% of insulin release within 100 min <i>in vitro</i>.</li> <li>● The Nanoparticles demonstrated no significant toxicity in GI cells after being treated for 3 h.</li> <li>● Methylated N-(4-N, N-dimethylaminobenzyl) chitosan Nanoparticles elicited higher insulin absorption than trimethyl chitosan Nanoparticles.</li> </ul>	2014: [8]
Insulin-loaded chitosan/arabic gum	Ionotropic gelation	2 <sup>3</sup> factorial design	<ul style="list-style-type: none"> <li>● High level of initial burst release (30% to 50%) within 15 min at acidic pH.</li> <li>● Nanoparticles could facilitate the</li> </ul>	2011: [12] 2010: [54]

Nanoparticles			transportation of insulin <i>ex vivo</i> .	
Insulin-loaded modified chitosan Nanoparticles	Polyelectrolyte complexation	D-optimal response surface methodology	<ul style="list-style-type: none"> <li>● A slight increase in particle size as the concentrations of methylated (aminobenzyl), methylated (benzyl) and methylated (pyridinyl) chitosan increase.</li> <li>● The polymer concentration had significant effect on the zeta potential of Nanoparticles.</li> <li>● As the concentration of polymer increases, the polydispersity index of the Nanoparticles increases.</li> <li>● Polymer type had significant effect on the polydispersity index of the Nanoparticles.</li> <li>● Burst release of insulin was presented by the fabricated Nanoparticles with at least 20% to 40% of insulin release within 50 min.</li> </ul>	2011: [55]
Insulin-loaded chitosan/albumin-coated alginate/dextran Nanoparticles	Ionotropic gelation	Box Behnken design	<ul style="list-style-type: none"> <li>● Particle size was dependent on the concentration of calcium chloride, chitosan and albumin.</li> <li>● Polydispersity index was dependent on the calcium concentration, but not the concentration of chitosan or albumin.</li> <li>● Zeta potential was influenced by the concentration of chitosan due to the existence of positively charged amino groups.</li> <li>● The drug release property was dependent on the chitosan concentration due to the swelling property of chitosan.</li> <li>● The drug release property was also dependent on the concentration of the albumin concentration due to its effect on the strength of electrostatic interaction.</li> <li>● Burst release of insulin from the Nanoparticles was observed at the alkaline pH with more than 80% release after 180 min.</li> </ul>	2009: [56]
Insulin-loaded poly-epsilon-caprolactone/ Eudragis RS1 Nanoparticles	Water-in-oil-in-water emulsification and evaporation method	D-optimal response surface methodology	<ul style="list-style-type: none"> <li>● As the ratio of poly(epsilon caprolactone) to Eudragit RS decreases, the particle size decreases due to the surfactant behaviour of Eudragit RS.</li> <li>● As the ratio of poly(epsilon caprolactone) to Eudragit RS increases, the polydispersity increases.</li> <li>● An initial burst release of insulin was observed, followed by controlled drug release for 7 h.</li> </ul>	2005: [57]

**Table 2.** Mean particle size, polydispersity index and zeta potential of insulin-loaded CS-Dz13Scr nanoparticles/microparticles.

	Formulations		Physical characteristics		
	CS concentration	Dz13Scr amount	Particle size $\pm$ S.D (nm)	Polydispersity index $\pm$ S.D	Zeta potential $\pm$ S.D (mV)
1.	0.00004%	5 $\mu$ g	377.3 $\pm$ 61.6	0.500 $\pm$ 0.179	-1.84 $\pm$ 1.13
2.		10 $\mu$ g	290.4 $\pm$ 39.0	0.460 $\pm$ 0.027	-0.70 $\pm$ 0.30
3.		15 $\mu$ g	832.9 $\pm$ 525.2	0.893 $\pm$ 0.186	-0.90 $\pm$ 0.25
4.	0.00025%	5 $\mu$ g	245.3 $\pm$ 240.6	1 $\pm$ 0	-0.81 $\pm$ 0.63
5.		10 $\mu$ g	2341.8 $\pm$ 2414.4	0.764 $\pm$ 0.206	-1.21 $\pm$ 0.51
6.		15 $\mu$ g	419.9 $\pm$ 75.9	0.439 $\pm$ 0.067	-0.82 $\pm$ 0.74
7.	0.0004%	5 $\mu$ g	382.4 $\pm$ 84.9	0.758 $\pm$ 0.212	-1.02 $\pm$ 0.75
8.		10 $\mu$ g	380.0 $\pm$ 242.8	0.666 $\pm$ 0.282	-2.68 $\pm$ 2.98
9.		15 $\mu$ g	516.8 $\pm$ 328.7	0.712 $\pm$ 0.033	-0.53 $\pm$ 0.08
10.	0.0025%	5 $\mu$ g	267.7 $\pm$ 34.6	0.313 $\pm$ 0.133	-1.00 $\pm$ 0.55
11.		10 $\mu$ g	234.6 $\pm$ 41.7	0.283 $\pm$ 0.050	-0.56 $\pm$ 0.25
12.		15 $\mu$ g	201.0 $\pm$ 95.7	0.421 $\pm$ 0.209	-0.41 $\pm$ 0.03
13.	0.004%	5 $\mu$ g	662.2 $\pm$ 69.4	0.497 $\pm$ 0.038	-10.12 $\pm$ 2.81
14.		10 $\mu$ g	159.3 $\pm$ 8.7	0.331 $\pm$ 0.001	-1.08 $\pm$ 0.36
15.		15 $\mu$ g	203.4 $\pm$ 74.0	0.409 $\pm$ 0.155	-0.80 $\pm$ 0.75
16.	0.025%	5 $\mu$ g	4669.3 $\pm$ 3231.2	0.247 $\pm$ 0.122	-12.12 $\pm$ 3.35
17.		10 $\mu$ g	1942.3 $\pm$ 322.1	0.897 $\pm$ 0.047	-14.20 $\pm$ 2.21
18.		15 $\mu$ g	1566.7 $\pm$ 345.8	0.464 $\pm$ 0.182	-21.27 $\pm$ 1.21
19.	0.04%	5 $\mu$ g	1109.7 $\pm$ 11.0	0.575 $\pm$ 0.095	5.17 $\pm$ 0.26
20.		10 $\mu$ g	6428.3 $\pm$ 565.1	0.521 $\pm$ 0.426	-9.54 $\pm$ 1.58
21.		15 $\mu$ g	3652.3 $\pm$ 1706.6	0.723 $\pm$ 0.279	-16.90 $\pm$ 1.28
22.	0.25%	5 $\mu$ g	655.7 $\pm$ 20.8	0.429 $\pm$ 0.005	8.17 $\pm$ 0.34
23.		10 $\mu$ g	718.5 $\pm$ 24.2	0.504 $\pm$ 0.029	9.69 $\pm$ 0.81
24.		15 $\mu$ g	595.3 $\pm$ 14.3	0.495 $\pm$ 0.037	10.97 $\pm$ 0.75

**Table 3.** The main effect, significant coefficients, impact of main and interaction parameters on the outcome responses (size, polydispersity index, zeta potential) for insulin-loaded CS-Dz13Scr particles.

Formulations	Independent factors	Dependent variables	Summary of main findings
Insulin-loaded CS-Dz13Scr particles	X <sub>1</sub> polymer concentration (0.00004, 0.00025, 0.0004, 0.0025, 0.004, 0.025, 0.04 or 0.25% chitosan in 25 mM SA buffer; 100 µl)	Size	<ul style="list-style-type: none"> <li>● F = 5.33 (p = 0.0035)</li> <li>● <b>Main effects:</b> chitosan concentration</li> <li>● <b>Significant coefficients:</b> chitosan concentration (p &lt; 0.0001)</li> <li>● <b>Coefficients that reduce size:</b> Dz13Scr amount, chitosan concentration (quadratic term), Dz13Scr amount (quadratic term)</li> <li>● <b>Coefficients that increase size:</b> chitosan concentration, interaction between chitosan and Dz13Scr</li> </ul>
		Polydispersity index	<ul style="list-style-type: none"> <li>● <b>Main effects:</b> chitosan concentration</li> <li>● <b>Coefficients that reduce pdi:</b> chitosan concentration, chitosan concentration (quadratic term)</li> <li>● <b>Coefficients that increase pdi:</b> Dz13Scr amount, interaction between chitosan and Dz13Scr, Dz13Scr amount (quadratic term)</li> </ul>
		Zeta potential	<ul style="list-style-type: none"> <li>● F = 5.19 (p = 0.004)</li> <li>● <b>Main effects:</b> chitosan concentration</li> <li>● <b>Significant coefficients:</b> chitosan concentration (p = 0.0059), chitosan concentration (quadratic term; p = 0.0017)</li> <li>● <b>Coefficients that reduce zeta potential:</b> Dz13Scr amount, Dz13Scr amount (quadratic term)</li> <li>● <b>Coefficients that increase zeta potential:</b> chitosan concentration, interaction between chitosan and Dz13Scr, chitosan concentration (quadratic term)</li> </ul>



**Figure 1.** Schematic presentation of the preparation and pharmaceutical analysis of insulin-loaded nanoparticle.

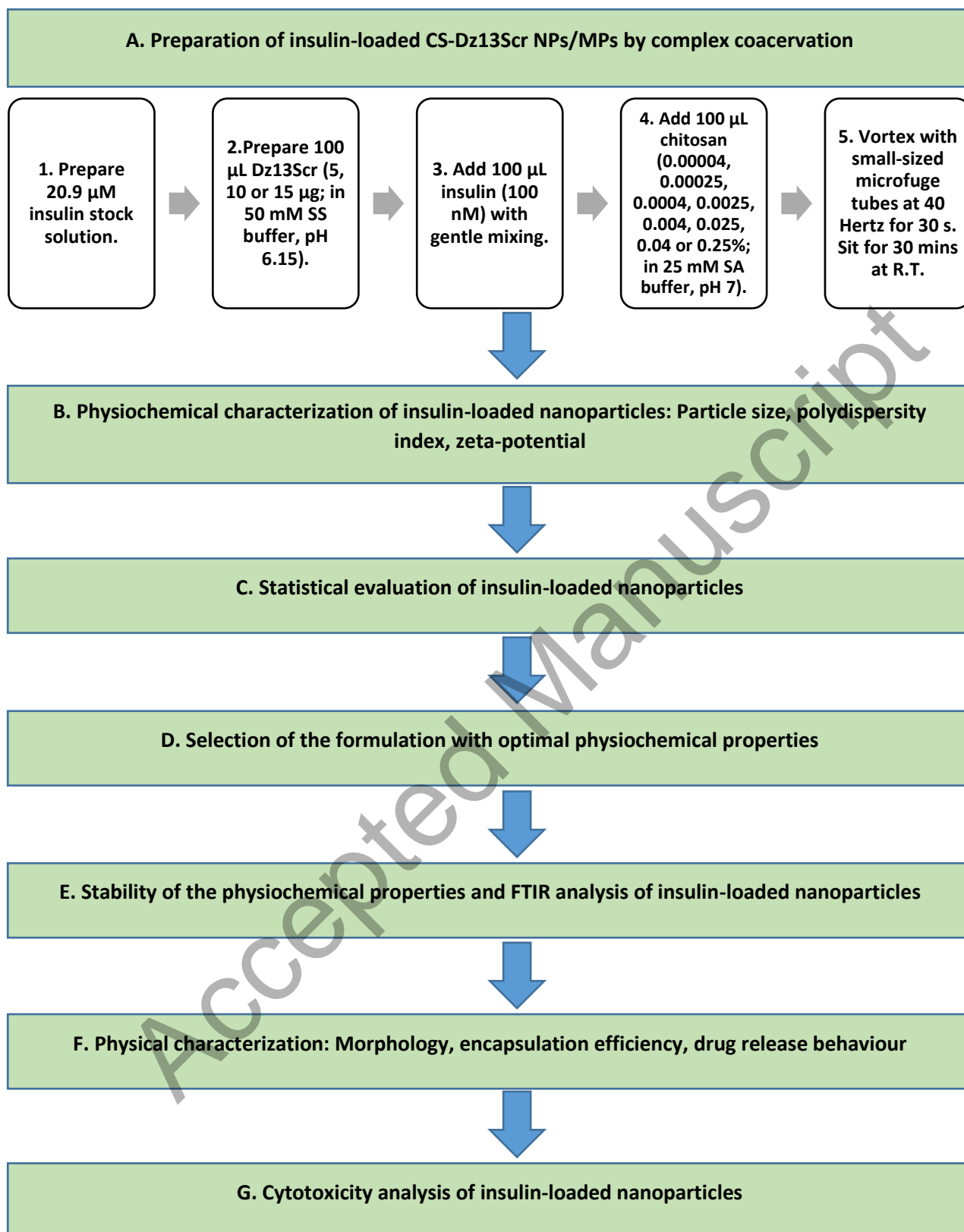


**Figure 2.** The particle size, polydispersity index and zeta potential of insulin-loaded particles.

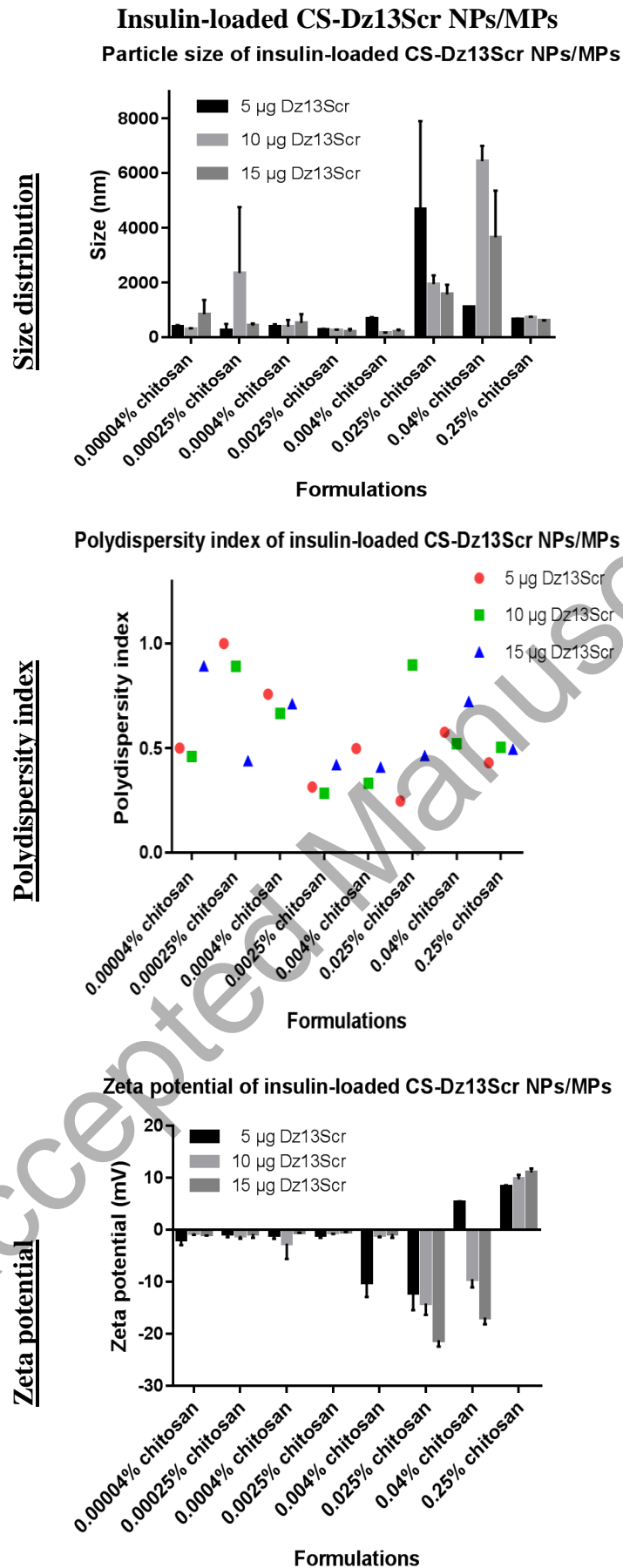


**Figure 3.** The response surface plot of insulin-loaded CS-Dz13Scr particles for size distribution, polydispersity index and zeta potential.

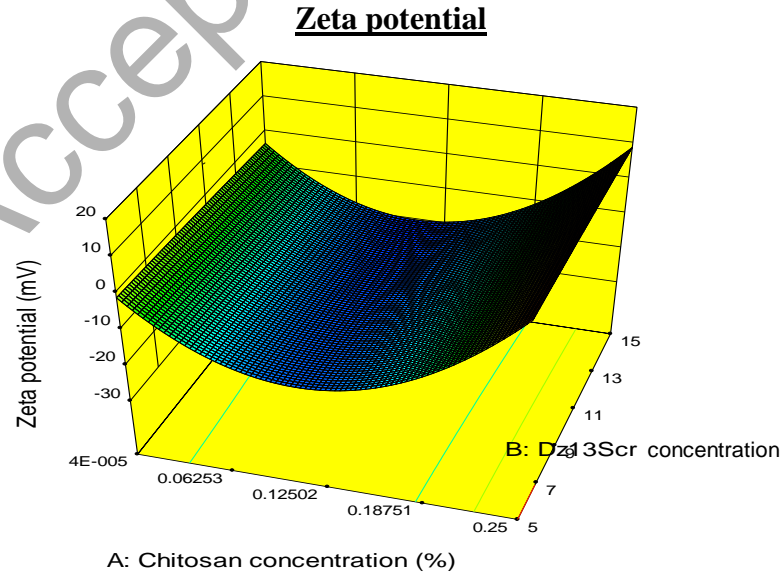
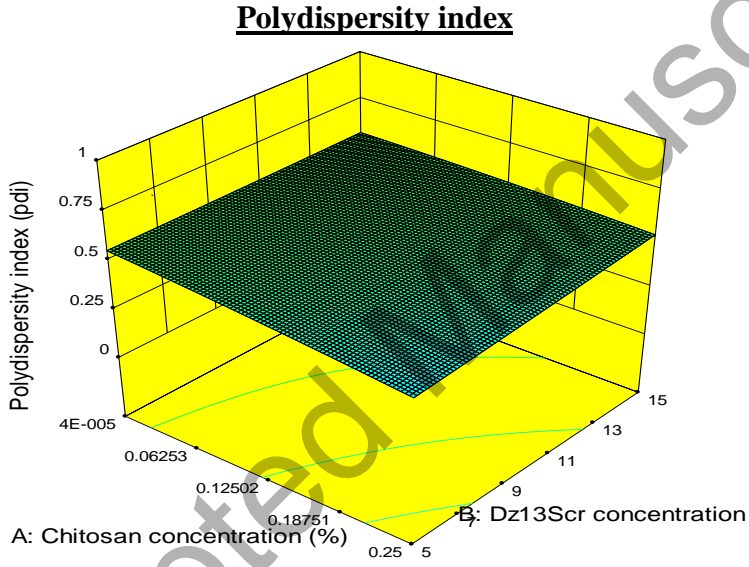
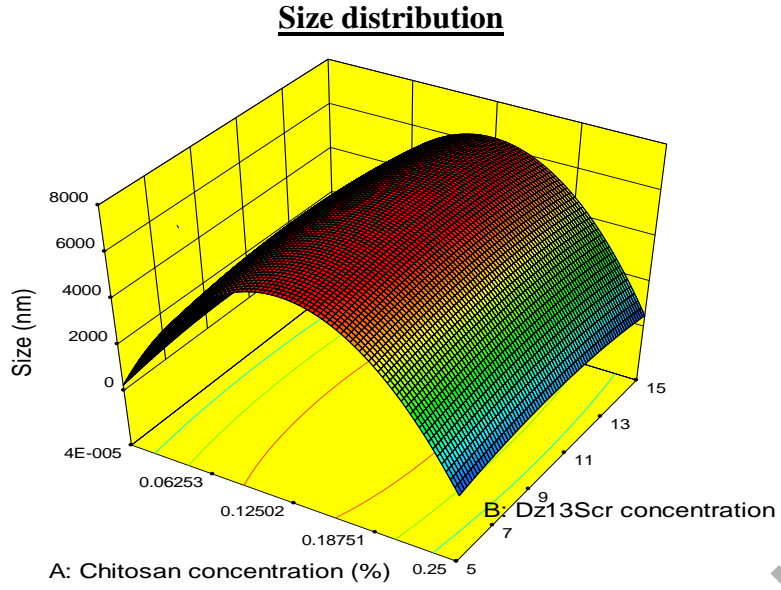


**Figure 4.** The stability of physicochemical properties and FTIR spectra of insulin-loaded nanoparticles.

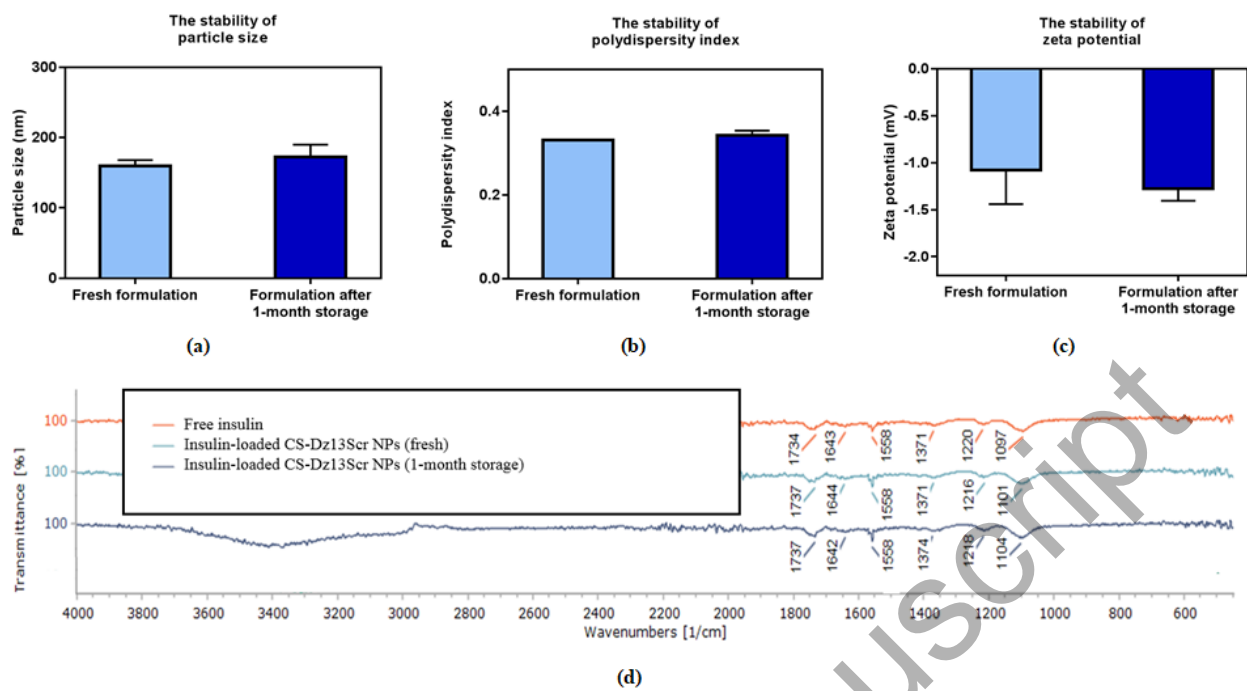


**Figure 5.** The SEM image and drug release profile of insulin-loaded CS-Dz13Scr nanoparticles.

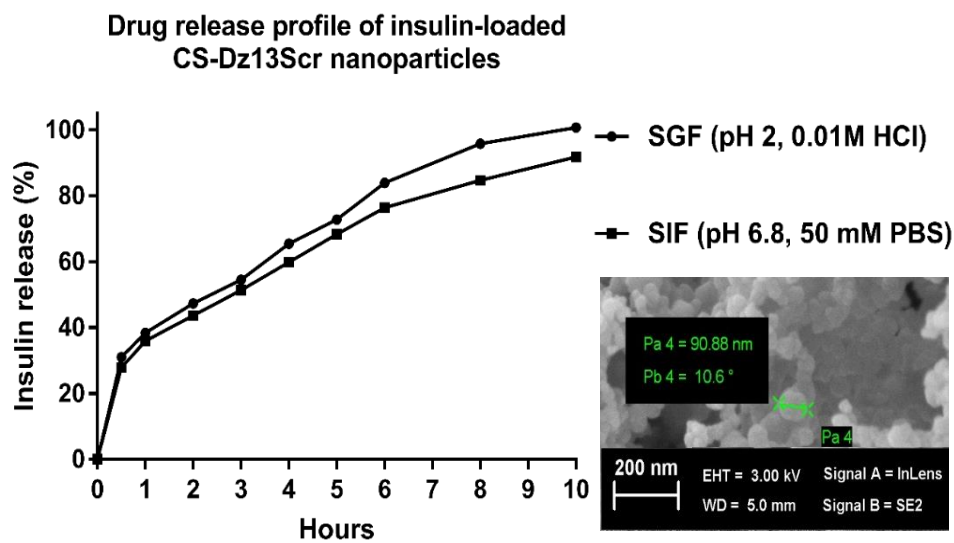


**Figure 6.** The cell viabilities of HT29 cells and C2C12 cells.

